# A Complex Automata approach for In-stent Restenosis: two-dimensional multiscale modeling and simulations

Alfonso Caiazzo [b] and David Evans [c] , Jean-Luc Falcone [d] ,
Jan Hegewald [e] , Eric Lorenz [f] , Bernd Stahl [d] , Dinan Wang [g] ,
Jörg Bernsdorf [h] , Bastien Chopard [d] , Julian Gunn [c] ,
Rod Hose [c] , Manfred Krafczyk [e] , Pat Lawford [c] ,
Rod Smallwood [c] , Dawn Walker [c] , Alfons Hoekstra [f]

[a] *INRIA Rocquencourt, BP 105, F-78153 Le Chesnay Cedex, France*

[b] *WIAS Berlin, Mohrenstr. 39, D-10117 Berlin, Germany*

[c] *The University of Sheffield, Beech Hill Road, S10 2RX, Sheffield, UK*

[d] *University of Geneva, CUI, Departement d'Informatique,
Battelle Bat. A, 7 route de Drize, CH-1227 Carouge, Switzerland*

[e] *Technische Universität Braunschweig,
Pockelsstr. 3, 38106 Braunschweig, Germany*

[f] *University of Amsterdam, Kruislaan 403, 1098 SJ Amsterdam, the Netherlands*

[g] *Meteorological Institute, University of Bonn,
Auf dem Hügel 20, 53121 Bonn, Germany*

[h] *German Research School for Simulation Science GmbH,
Schinkelstr. 2a, 52062 Aachen, Germany*

## Abstract

In-stent restenosis, the maladaptive response of a blood vessel to injury caused by the deployment of a stent, is a multiscale system involving a large number of biological and physical processes. We describe a Complex Automata Model for in-stent restenosis, coupling bulk flow, drug diffusion, and smooth muscle cell models, all operating on different time scales. Details of the single scale models and of the coupling interfaces are described, together with first simulation results, obtained with a dedicated software environment for Complex Automata simulations. Preliminary results show that the model can reproduce growth trends observed in experimental studies and facilitate testing of hypotheses concerning the interaction of key factors.

*Key words:* Complex Automata, in-stent Restenosis, Multiscale Modeling, Agent Based Models.

# 1 Introduction

A *stenosis* is a narrowing of a blood vessel lumen due to the presence of an atherosclerotic plaque. This can be corrected by balloon angioplasty, after which a *stent* (metal mesh) is deployed to prevent the vessel from collapsing. The injury caused by the stent can lead to a maladaptive biological response of the cellular tissue (mainly due to smooth muscle cell proliferation). The abnormal growth can produce a new stenosis (re-stenosis).

Restenosis develops under conditions of pulsatile flow and there exists an interaction between the much studied biological pathways and those of a physical nature [12,21]. The multiscience and multiscale nature of in-stent restenosis has been discussed in detail previously by Evans et al. [7].

The design and geometry of the stent employed influences the biological events occurring in the vessel following deployment. Strut thickness, number, cross-sectional shape and arrangement, and stent length all influence the haemodynamics and degree of injury and stretch observed within the stented segment [22]. These in turn, are critical determinants of the severity of restenosis observed. Additionally, stents may be coated with active compounds targeted at the biological processes responsible for driving the progression of restenosis which, when eluted locally at the stented site, can prevent proliferation of smooth muscle cells and neointimal growth.

The development of a multiscale *in silico* model capable of testing both the influence of stent geometry and that of drug elution is motivated by the desire for a better understanding of the dynamics regulating restenosis. Thus providing a potentially powerful tool for improved understanding of the biology, and to assist in the process of device/therapy development.

As in many other biological systems, the dynamics of in-stent restenosis span many orders of magnitude through the scales, from the smallest microscopic scales up to the largest macroscopic ones. The wealth of experimental data

*Email addresses:* `caiazzo@wias-berlin.de` (Alfonso Caiazzo), `david.evans@sheffield.ac.uk` (David Evans), `jean-Luc.Falcone@unige.ch` (Jean-Luc Falcone), `hegewald@irmb.tu-bs.de` (Jan Hegewald), `e.lorenz@uva.nl` (Eric Lorenz), `bernd.stahl@unige.ch` (Bernd Stahl), `dinanbonn@yahoo.de` (Dinan Wang), `j.bernsdorf@grs-sim.de` (Jörg Bernsdorf), `bastien.chopard@unige.ch` (Bastien Chopard), `j.gunn@sheffield.ac.uk` (Julian Gunn), `d.r.hose@sheffield.ac.uk` (Rod Hose), `kraft@irmb.tu-bs.de` (Manfred Krafczyk), `p.lawford@sheffield.ac.uk` (Pat Lawford), `r.smallwood@sheffield.ac.uk` (Rod Smallwood), `d.c.walker@sheffield.ac.uk` (Dawn Walker), `a.g.hoekstra@uva.nl` (Alfons Hoekstra).

that is now available has made *in silico* experimentation an attractive tool in systems biology, allowing hypothesis testing and formulation of predictions which can be further tested *in vitro* or *in vivo* [19]. In recent years the computational biology community has developed extremely powerful methods to model and simulate fundamental processes of a natural system on a multitude of separate scales. The next challenge is to study, not only fundamental processes, on all these separate scales, but also their mutual coupling across the scales and to determine the emergent structure and function of the resulting system [25].

Despite the large body of literature on multiscale models, the key feature of multiscale modelling, the actual coupling between scales is still at a very early stage of development [14,26].

In this context, Complex Automata (CxA) have recently been introduced as a paradigm to simulate multiscale systems as a collection of single scale models, interacting across the scales [14,15,16].

Based on the conceptual description of the relevant processes and their characteristic temporal and spatial scales which has been presented in [7], we describe a simplified CxA model of the multiscale process, coupling a *lattice Boltzmann* bulk flow (BF) solver (for the blood flow), an *agent based model* for smooth muscle cell (SMC) dynamics (simulating cell growth, the cell cycle, physical and biological cell-cell interaction), and a *Finite Difference scheme* for the drug diffusion (DD) within the cellular tissue.

In section 2 we introduce the main ideas behind the CxA approach. Section 3 discusses how coupling between models has been realised using a CxA dedicated software environment [1,13]. In section 4, following a short introduction on in-stent restenosis, we present the multiscale model. We describe the main characteristics of the single scale solvers, which have been developed independently from each other, and independently from the ultimate application. We also describe, in detail, the coupling of the single-scale solvers with relevance to this particular application. Preliminary simulation results are presented in section 5 and conclusions are discussed in section 6.

## 2   Complex Automata Modeling

Recently we proposed Complex Automata (CxA) as a paradigm for multiscale modelling and simulation [14,15,16]. CxA theory dictates that a multiscale system can be decomposed into mutually interacting single scale models.

The multiscale system, and its formulation as a CxA can be represented graph-

ically on a **Scale Separation Map** (SSM), where the horizontal and vertical axes represent the temporal and spatial scales. An example of such a SSM (as discussed in detail in section 4) is shown in fig. 1. Here, the system (represented by a large area on the SSM) has been decomposed into three interacting sub-processes (single scale models) and their interactions.

**Single Scale Models.** The single scale models are discrete processes and explicitly update their state in time using a well defined evolution operator, in the form of *collision+propagation*

The collision-propagation terminology is borrowed from the lattice gas automata framework (for example, see [4]), and has recently been shown to be equivalent to other update paradigms [5].

This methodology is not restrictive, as it allows construction of single scale models using a large class of numerical methods (e.g. Cellular Automata, Lattice Boltzmann Methods, Agent Based Models, Finite Difference). Moreover, consideration of a class of algorithms with well specified evolution rules allows one to formally define a single scale model through a tuple [14,15,16],

$$\mathcal{C} = \{A(\Delta x, L, \Delta t, T), \mathbb{F}, \Phi_{\Delta x, \Delta t}(\mathbf{P}, \mathbf{C}), \mathbf{O}\}. \tag{1}$$

where $A$ is the computational domain, made (in space) of cells of size $\Delta x$, spanning a region of size $L$, and (in time) of steps of size $\Delta t$ over an interval $[t_0, t_0 + T]$ (represented on the SSM, see figure 1). $\mathbb{F}$ is the discrete space of the numerical solution (space of states), $\Phi : \mathbb{F} \rightarrow \mathbb{F}$ is the update rule defined through propagation and collision operators ($\mathbf{P}$ and $\mathbf{C}$) and dependent on $\Delta x$, $\Delta t$. Finally, we associate an *observable*, i.e. an operator $\mathbf{O} : \mathbb{F} \rightarrow \mathbb{R}^d$ to each algorithm.

**Coupling templates.** An essential step in the modelling process is the inclusion of specific *coupling templates*, designed to mimic the dynamic behavior of the multi-scale process as accurately as possible. In the CxA formulation, a coupling template between two single scale models can be formally expressed as an interaction between the *observable* of the first, and the execution loop (i.e. initial conditions, collision, boundary condition operators) of the second model.

## 3 CxA Simulation Framework: Multiscale Coupling Library and Environment

The conceptual ideas behind the CxA approach (decomposition into single scale models, restriction to a common instruction flow and specification of finite number of coupling templates) have been used to develop the COAST
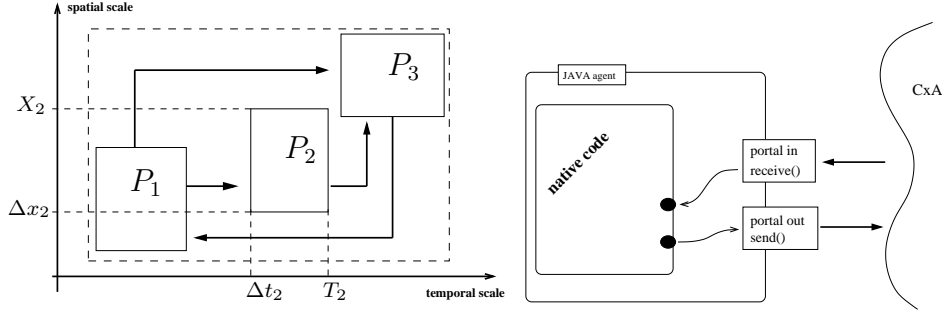
Figure 1. Left: Example of SSM: a multiscale process (box with dashed edges) has been decomposed into 3 coupled single scale models. Right: Native Codes can be connected "wrapped" as JAVA agents (kernels), and coupled to a CxA using MUSCLE, including *portals* with the framework. The `send()` and `receive()` operations are performed within these portals.

*Multiscale Coupling Library and Environment* (MUSCLE) [1,13], a software environment in which a CxA can be implemented naturally.

Within the coupling library, both the kernels (i.e. the single scale models) and the conduits (i.e. the multiscale coupling) are software agents of the underlying multiagent platform JADE (`www.jade.tilab.com`).

Kernels and conduits (conceptually central to the CxA modeling language) communicate using two communication primitives:

- A non-blocking `send` operation, to send data from a kernel to a conduit entrance. It returns as soon as the data is sent to the conduit.
- A blocking `receive` operation, to allow a kernel to receive data from the exit of a conduit. The receiving kernel waits until the data is available before computations are resumed.

The single scale models do not need to be aware of each other and the information on the coupling and the global setup are held by the framework. This allows the implementation of complex interfaces, where multiscale couplings can be performed by the use of smart conduits.

Furthermore, the structure of the coupling library allows complete independence from native codes. These can be replaced with a different source, provided the interface with respect to the framework (i.e. the JAVA-wrapper agent) remains the same. In the particular example of in-stent restenosis, described in section 4, three single scale models have been implemented in different programming languages (FORTRAN90, C++, JAVA), wrapped as JAVA agents, and connected via the MUSCLE framework (figure 1, right). The details of coupling for this particular application are discussed in section 4.2.
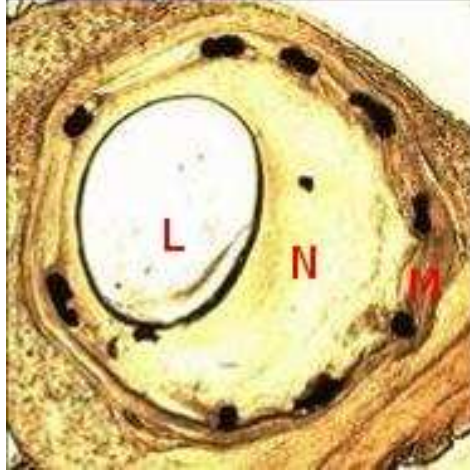
Figure 2. A stented coronary artery showing a significant restenosis due to neointimal growth (N) into the lumen (L). Stent struts are clearly visible and penetrate the original vessel wall (M).

## 4 Multiscale Model of In-stent Restenosis

Restenosis, can be loosely described as a 'loss of gain' - that is, a late return of the vessel lumen to a size similar to that seen before intervention (stent deployment; see figure 2). It has, historically, been considered as a over reaction of the general wound healing response within vascular tissue [9]. From a biological standpoint, injury caused by stent deployment (during balloon inflation) is thought to trigger a cascade of inflammatory events, that ultimately results in the development of new tissue (the neointima) [8,23].

The majority of investigations into this phenomenon consider the biological and physical processes involved independently when, in fact, there is a complex interplay between the two. Blood flow, biological events (e.g. inflammation), stent geometry, drug elution and diffusion all influence the overall response of the the artery wall to stent deployment. The aim of the CxA model is to improve our understanding of this complex system by considering restenosis explicitly as a multiscale multiscience system.

Following an in depth literature review, the processes key to the regulation of restenosis were identified, and their temporal and spatial scales determined. Coupling was considered in terms of the interactions between these processes. This allowed us to generate a comprehensive conceptual scale separation map [7], defining a CxA, containing the sub-models necessary to capture the behavior of the system, and depicting the coupling between them; i.e. the flow of information between models.

The first practical implementation of the CxA reported herein considers a simplified version of the model focusing on SMC behavior, and its interaction
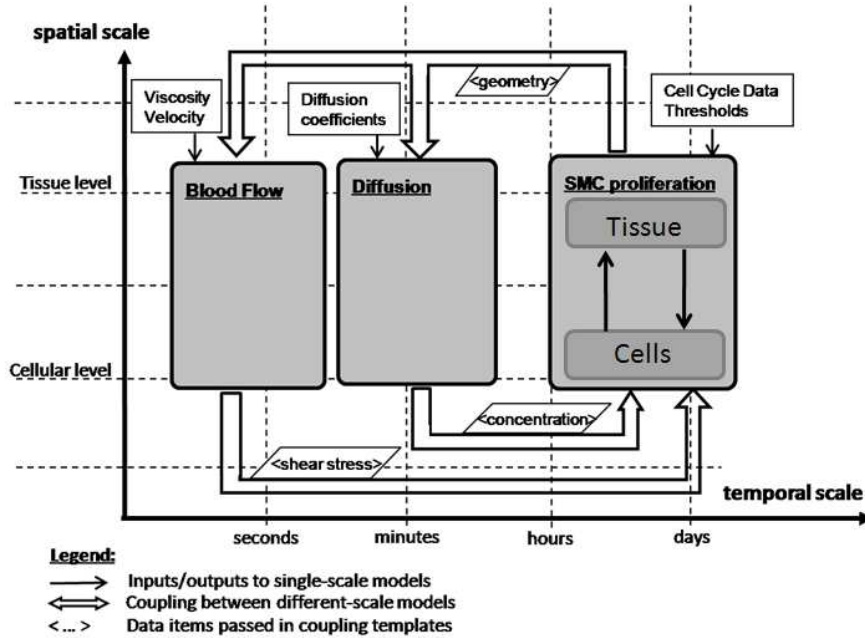
Figure 3. The simplified SSM, depicting the three single scale models and their mutual coupling.

with blood flow and drug eluted from the stent. The simplified SSM is shown in figure 3.

Following deployment of the stent, which is modelled as a separate process to provide an initial condition (using the SMC model itself, see section 5.1), SMCs start to proliferate in response to the mechanical insult. The rate of smooth muscle cell proliferation is dependent on the blood flow (specifically wall shear stress (WSS) and oscillatory stress index (OSI)), the number of neighbouring smooth muscle cells, and in the case of a drug eluting stent, the local concentration of drug. The blood flow, in turn, depends on the lumenal geometry (and thus changes with the proliferation of SMCs), and the concentration of drug depends on the SMC/tissue domain (and therefore also on SMC proliferation). In the current model we assume that scale separation between the single scale models is confined to the temporal scale, however it is worth noting that scale separation on a spatial scale exists within the SMC model itself. The SMC model can sub-divided into the processes which occur on the cellular level, and those occurring on the level of the tissue, resulting in a hierarchical CxA model. The SMC proliferation is the slowest process, dictated by the cell cycle, whereas flow is a fast process, dictated by the length of one cardiac cycle. Due to the specific value of the diffusion coefficients and the typical spatial dimensions of the arterial tissue, the temporal scale of the diffusion process resides between that of flow and SMC scales. In future models we will also explicitly consider spatial scale separation.

7
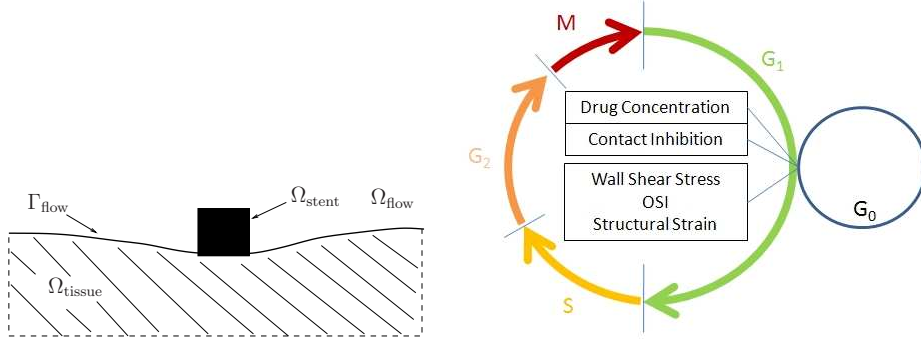
Figure 4. Left: The 2D computational domain is divided into vessel lumen, tissue and stent struts. Right: the cell cycle model, based on three stages (**G0**,**G1**, **S/G2/M**) and a biological ruleset.

## 4.1 Single Scale Models and Coupling Templates

In this section, the technical details of the CxA model of in-stent restenosis are presented in brief. We first describe the *kernels* of the CxA, i.e. the algorithms used to simulate the single scale models (Bulk Flow , SMC Behavior and Drug Diffusion). The native codes of these have been constructed independently from the multiscale application. Then, we show how these elements are connected via *smart conduits* using a CxA dedicated coupling library [1] (see section 3).

### 4.1.1 Bulk Flow Solver (BF)

Blood flow is modelled as a Newtonian incompressible fluid governed by incompressible Navier-Stokes equations

$$
\begin{aligned}
&\rho_0 \partial_t \mathbf{u} + \rho \mathbf{u} \cdot \nabla \mathbf{u} + \nabla p = \rho \nu \nabla^2 \mathbf{u} + \mathbf{f}, \ t > 0, \ \mathbf{x} \in \Omega_{\text{flow}}(t) \\
&\nabla \cdot \mathbf{u} = 0, \ t > 0, \ \mathbf{x} \in \Omega_{\text{flow}}(t) \\
&\mathbf{u}(t, \mathbf{x}) = 0, \ \mathbf{x} \in \Gamma_{\text{flow}}(t)
\end{aligned}
\tag{2}
$$

where $\rho_0$ is the blood density, $\nu$ is the viscosity, assumed constant in the Newtonian approximation (a commonly accepted hypothesis for large vessels). The set $\Omega_{\text{flow}}(t)$ represents the lumen domain, with $\Gamma_{\text{flow}}(t)$ being its interface with the tissue domain. Equation (2) has to be completed with appropriate inlet-outlet boundary conditions, which may vary depending on the focuses of the model.

To obtain a numerical solution of (2), we employ a Lattice Boltzmann Method (LBM), which, unlike other CFD approaches, approximates the hydrodynamics starting from a pseudo-microscopic description of the fluid. In detail, the spatial domain is discretized using a regular square lattice $\mathcal{L}(h)$, of spacing $h$, and the so-called D2Q9 set of discrete velocity vectors $\{h\mathbf{c}_i, i = 1, \ldots, b\}$,

8

connecting neighboring nodes of the lattice. For the problem presented here, we chose $h = 0.01$ cm, which roughly correspond to having 10 grid points per strut side, in order to resolve with sufficient accuracy the flow patterns near the boundary.

At each node $\mathbf{x} \in \mathcal{L}(h)$, and at each time step $t$, the unknowns are the distributions $f_i(t, \mathbf{x})$, representing the density of particles traveling in direction of $\mathbf{c}_i$. Given the time step $\Delta t$, and with $\Delta x = h$, the evolution in time of the variables $f_i$ reads

$$f_i(t + \Delta t, \mathbf{x} + \Delta x \mathbf{c}_i) = f_i(t, \mathbf{x}) + J_i(f(t, \mathbf{x})). \tag{3}$$

The right hand side defines the *collision operator*, which depends on the viscosity $\nu$ in (2). For detailed overviews of the LBM, we refer the reader to [2,3,4,27].

In our first simulations, we used a standard BGK collision model. The Dirichlet boundary condition on the interface $\Gamma_{\text{flow}}(t)$ has been imposed through bounce-back rule, while periodic boundary conditions has been used at inlet and outlet. In this case, an appropriate volume force $\mathbf{g}$ has been added to simulate a pressure gradient through the domain. It is important to remark that particular implementation choices (as collision operator, boundary conditions, body-forcing) or optimization techniques such as parallelization or grid refinement might not be relevant for the multiscale model itself, as long as the physical problem is correctly approximated. At the same time, the coupling library and the coupling template are completely flexible with respect to the single scale solver, as long as the correct data interface is maintained.

The observable related to the BF single scale model is the wall shear stress on the vessel boundary (WSS), which is needed as input for the SMC model, after being properly mapped from the cartesian lattice on the individual cells.

### 4.1.2 Smooth Muscle Cells Dynamics (SMC)

The dynamics of the smooth muscle cells are simulated using an Agent Based Model. Each single cell is represented by agent, which is identified by a set of state-variables: *position, radius, biological state, drug concentration and structural stress*. Each SMC agent evolves in time according its own current state, and to the states of neighbouring cells. Each time step involves a physical solver, simulating the structural dynamics of cells, and a biological solver, which simulates the cell cycle, according to a biological rule set.

**Physical solver** From the structural point of view, 2D cells are represented by their centers, and a potential function, which determines non-linear re-

pulsive and attractive inter-cell forces. In addition, boundary forces, viscous friction, radial elastic forces (modeling the primary fibre direction of SMCs in a physiologically relevant 3D environment) and motility forces (modeling cell migration) are taken into account.

Neglecting inertial terms, the model is described by the system of equations

$$C\frac{d\mathbf{x}}{dt} = \mathbf{F}(t, \mathbf{x}, r) = \mathbf{F}_{\mathrm{rep}}(t, \mathbf{x}, r) + \mathbf{F}_{\mathrm{att}}(t, \mathbf{x}, r) + \mathbf{F}_{\mathrm{el}}(t, \mathbf{x}) + \mathbf{F}_{\mathrm{bound}}(t, \mathbf{x}), \quad (4)$$

where $\mathbf{x}$ is the vector of cell displacements, $r$ is the vector of cell radii, and $C$ is a matrix of friction coefficients. The forces vectors include different types of cell-cell interaction. Attractive and repulsive forces ($\mathbf{F}_{\mathrm{att}}$ and $\mathbf{F}_{\mathrm{rep}}$) have been derived by simple geometrical arguments. Repulsion is based on Hertzian contact of two elastic cylinders, whilst cell-cell attraction is proportional to overlapping surfaces. Furthermore, $\mathbf{F}_{\mathrm{el}}$ denotes the forces exerted by the elastic lamina agents on neighboring cells, used to to simulate impenetrability, and $\mathbf{F}_{\mathrm{bound}}$ (boundary forces) denotes additional forcing terms used to take into account external tissue.

At each iteration step, new equilibrium positions of SMCs are computed by iterating a finite difference scheme until a steady state is reached. Then, a surrogate of structural stress is then calculated and provided as input to the biological solver. In the current model, a simple Euler method is employed for the time integration of (4), but higher order Runge-Kutta schemes could also be employed. We found that the results do not depend on the particular choice of the integration scheme if the numerical parameters (i.e. time step and tolerance for the convergence criterion) are chosen properly. In particular, the time step was adaptively selected at each new iteration according to two criteria, (i) the eigenvalues of a simplified iteration matrix, and (ii) in order to bound the maximum displacement allowed for a single cell (of the order of 10% of cell radius). Moreover, the Euler scheme is significantly more compatible, as it can be naturally written in the collision+propagation form.

**Biological solver**  Each SMC agent progress through a cell cycle, modeled through a discrete set of states: quiescent state **G0**, a growth state **G1** and a *mitotic* state **S/G2/M**, i.e. when a *mother* cell divides into two new *daughter* cells (see figure 4).

Progression through the cell cycle takes place at a fixed rate, depending on the time step, culminating in *mitosis*. Cells may enter or leave an inactive phase of the cell cycle (G0) depending on certain rules based on contact inhibition, structural stress, and local drug concentration (received as input from the DD model).

The contact inhibition (CI) ruleset builds on the work of [28,29], started with the observation that cells in the centre of colonies epithelial cells (grown in a monolayer) become quiescent due to intercellular signalling which is mediated via *cadherin* cell-cell physical bonds. By implementing a CI rule, the authors saw a good qualitative fit between the computational epithelial growth model and the in vitro culture growth under similar conditions (with respect to calcium concentration). In the present SMC model, the contact inhibition rule was applied to SMCs within the vessel wall in, permitting the maintenance of quiescence in a densely packed, uninjured intact vessel wall.

In particular, the number of SMCs, IELs, and obstacle agents (e.g. the stent struts) within a certain range are computed. If the weighted sum exceeds a pre-determined threshold, the cell is contact inhibited. Additionally, cells are contact inhibited when they are closer to the outer surface of the tissue then the center of the nearest strut. This is designed to keep SMCs at the outer tissue surface quiescent, which would otherwise not emerge from the threshold count criterion since no outer lamina is modeled.

Cells can begin a proliferative stage also depending on their internal structural stress state (calculated computing all the forces acting on a cell in tangential and radial directions). In particular, if a previously quiescent cell were exposed to a stress exceeding a defined threshold, that cell would proceed to cell cycle entry and eventual proliferation. (this mechanism activate SMC response to the initial injury caused by stent deployment). **SHOULD WE SAY THAT THIS RULE WAS NOT USED? OR REMOVE THE PREVIOUS PARAGRAPH?**

Furthermore, for SMCs in contact with the fluid, rules are based on hydrodynamic parameters such as thresholds of wall shear stress (WSS) and oscillatory shear index[1] (OSI). These parameters are received as input from BF. In particular, low WSS, high OSI or high structural strain are individually capable of inducing agent proliferation if drug concentration and contact inhibition criteria allow.

### 4.1.3    Drug Diffusion in Cellular Tissue

Drug eluting stents represent an effective way of inhibiting neointima formation after stent-deployment. This process is captured in the present model through implementation of the Drug Diffusion (DD) kernel. Drug is eluted from the stent and diffuses into the cellular tissue. Thus the spatial domain for the DD kernel is coincident with that of the SMC.

---

[1]  The oscillatory shear index (OSI) measures the variability in time of tangential stresses. It is proportional to the ration between the mean value of the shear stress, in a period, and the average in time of its absolute value [10,18].

Biological tissues are heterogeneous in nature so we assume that this process can be described using a generic anisotropic diffusion law:

$$\partial_t c(t, \mathbf{x}) = \nabla \cdot (D_{\text{drug}} \nabla c(t, \mathbf{x}))$$
$$c(t, \mathbf{x}) = c_0, \ t > 0, \mathbf{x} \in \Omega_{\text{stent}} \tag{5}$$
$$c(t, \mathbf{x}) = 0, \ t > 0, \mathbf{x} \in \Gamma_{\text{flow}}(t)$$

where $c(t, \mathbf{x})$ is the concentration of the drug in the position $\mathbf{x}$ at time $t$, and $D_{\text{drug}}$ is the diffusion tensor.

In equation (5), $\Omega_{\text{stent}}$ denotes the part of a vessel occupied by the stent strut, $\Omega_{\text{tissue}}$ represents the tissue subdomain, and $\Gamma_{\text{flow}}$ corresponds to its interface with the flow domain.

Furthermore, we assume a complete time scale separation between flow and diffusion, in the sense that drugs eluted into the lumen are immediately and continuously flushed away by the faster blood. In (5), this is taken into account by a sink boundary condition on $\Gamma_{\text{flow}}$. On the other hand, stent struts act as a source.

In the practical algorithm, after discretization of the whole model geometry, mesh points are classified as *tissue*, *source* or *sink*. These are treated differently during the computation.

The diffusion tensor is chosen such that diffusion along the axis of the artery (or tangential to a cross section) is at least 10 times higher than diffusion in the radial direction [17,20].

To solve equation (5) numerically, we employ a Finite Difference (FD) approach which is solved using a Propagation-Collision loop[2], thus fitting with the the CxA modeling language.

According to [20], the time scale to reach the steady state is of the order of minutes (comparable with the SSM in figure 3). Therefore, when coupling DD and SMC, we are mainly interested in the steady drug concentration (the time step for the SMC model, which uses the drug concentration as input, is of the order of 1 day). In the context of this CxA model, this allows direct consideration of the simplified equation:

$$\nabla \cdot (D_{\text{drug}} \nabla c(t, \mathbf{x})) = 0 \tag{6}$$

---

[2] LB approaches for the diffusion equation could also be used. The choice of a FD scheme was dictated by two main arguments: (i) FD schemes in general need less memory than the LBM; (ii) the choice of a FD helped us to investigate and demonstrate the coupling of the different modeling approaches within the same CxA.
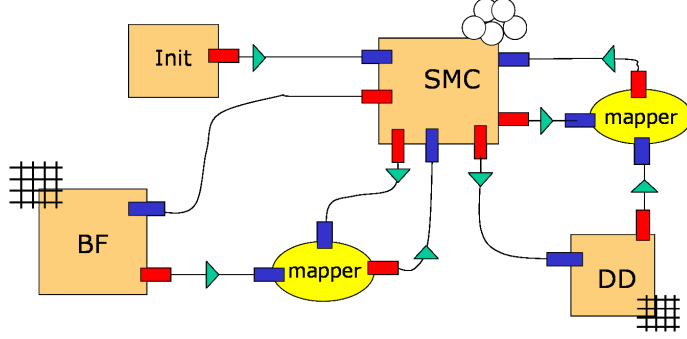
Figure 5. The Connection Scheme, showing the single scale models (Bulk Flow, SMC, Drug Diffusion), the Init agent (used to generate the initial structural stress condition in the tissue), the mapper agents and the conduits. Single scale models are mesh-based (BF, DD) or Agent-based (SMC).

(with appropriate boundary conditions).

*4.2    The In-stent Restenosis CxA: Kernels, Connection Scheme and Conduits*

In order to combine the single scale *kernels* described above using MUS-CLE [1], we need to define a communication graph, the *Connection Scheme* (CS), which specifies in detail the communication topology of the CxA, defining which pairs of kernels communicate. The Connection Scheme for the CxA model of in-stent restenosis is shown in figure 5.

In addition to BF, DD and SMC kernels, the current CxA setup includes a kernel which generates the initial conditions (IC) by simulating stent deployment into the cellular tissue (see section 5.1).

Multiscale coupling is implemented using special agents called smart conduits. Often, these perform *filtering* operations, converting output data from one single scale model to appropriate input for another. This is the case for geometrical couplings (through changes in the domains), when new SMC configurations (continuum based) are transformed into lattice based computational domains for BF and DD:

**Conduit: SMC to BF.** This conduit converts the array of positions and radii of cell agents, into a computational mesh for the flow solver which is decomposed into fluid and solid nodes.

**Conduit: SMC to DD.** Similarly, this conduit converts the array of positions and radii of the cells, into a computational mesh for the drug diffusion solver, marking the nodes as tissue, source, or sink.

In some instances, the interaction between kernels is slightly more complex,

and multiple inputs are required to compute one output. In these cases we introduce *mapper* agents (see figure 5). which, in the present CxA, are required whenever an input to the SMC model is generated:

**Mapper: BF to SMC.** The values of fluid shear stress at the boundary affect the biological evolution of the cells. Given the output of the bulk flow solver, and the current cell configuration, a mapper agent computes the shear stress on each cell. Depending on the discretization used for the flow solver, different approximation approaches can be used. If the flow grid is coarser than the spatial scale of the SMC model (the radius of the cells), an algorithm must be used in order to determine which cells are in contact with the flow, then the shear stress is extrapolated from the closest boundary fluid nodes for each cell position. On the other hand, if the flow discretization is sufficiently fine more fluid boundary nodes interact with a single cell and the shear stress on the cell surface can be calculated by averaging the values of the closest nodes.

**Mapper: DD to SMC** In this case, the drug concentration calculated in the DD has to be mapped to the SMC agents. Given the current drug concentrations and the SMC configuration, the mapper agent approximates the concentration on each cell. As for the shear stress approximation, the algorithm used depends on the grid size of the DD model. If the grid is fine enough (with many lattice nodes per SMC), the concentration on a cell can be integrated. If a coarse DD grid is used, the concentration for each cell is extrapolated using data from the closest nodes.

## 5    Simulation Results

### 5.1    Benchmark Geometry and Initial Conditions

As a benchmark geometry for the 2D CxA model, we consider a vessel, of length 1.5 mm and width 1.24 mm, where two square struts of side length 90 $\mu$m have been deployed. Dimensions of these 2D struts are matched to those of the *BiodivYsio* stent, which was used routinely in experimental works [11,6]. The width of the lumen was reduced to 1mm to make the coupled simulations computationally tractable in the available timescales.

The tissue geometry, in terms of medial (smooth muscle cell layer) thickness and cell/agent size, was also based on experimental conditions [11]. In particular, the vessel wall has a thickness of 120 $\mu$m. Smooth muscle cells are generated with an average radius of 15 $\mu$m and densely packed inside the wall.

Concerning the parameters for the biological solver, a WSS threshold taken
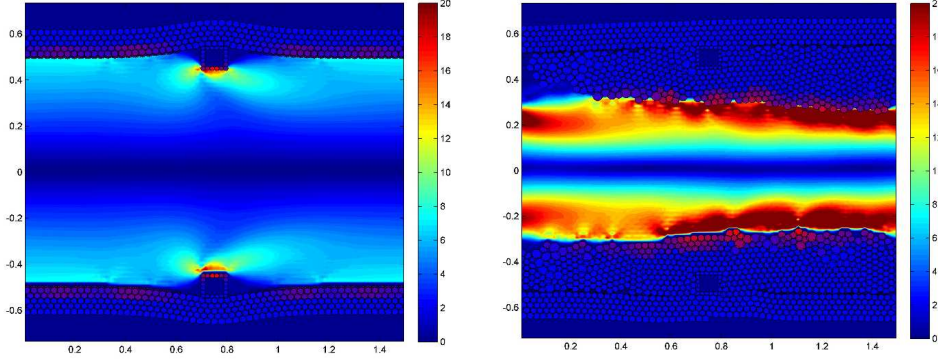
Figure 6. Left: Initial condition for the CxA model, including cell configuration, equilibrated after stent deployment, and the blood flow. Fluid shear stress is color coded (red high, blue low). Right: The same domain at 28 days post-stent deployment (672 iterations of the simulation). A neointima of SMC agents has developed in the lumen. Colour bars refer to the wall shear stress within the lumen in Pascals.

from the literature was adjusted appropriately to take into account the current vessel dimensions. In particular, a physiological threshold (for SMC proliferation) of 0.4 Pa in the real coronary geometry corresponds to a value of 2.76 Pa for the presented 2D CxA simulations if the global Reynolds number is conserved.

To obtain the initial condition based on the above geometry, an initial stress configuration compatible with the initial geometry must be provided. This initialization consists of two steps. First, an array of SMC agents, occupying the region of the artery wall with a given packing density is generated. Since this process can include a random assignation of cell sizes (within a fixed range) as well as some randomisation of position, the generated cells may not be in a state of equilibrium with their neighbours, based in the cell-cell interaction rules. The structural solver is operated with no external forces and the cells shuffle to an equilibrium state. Second, in order to generate the initial stress condition, stent deployment is modelled by computing the forces on the cells that come into contact with the stent as it is deployed. The direction of the force is normal to the surface of the stent and the magnitude is determined by the overlap of the stent with the cell in the same way as any other cellular contact. Additionally, since the artery wall has hoop (circumferential) stiffness, the deployment of the stent introduces a state of stress into the artery. This is implemented by application of a radial force on each cell that is a function of the radial displacement from the original geometry. The initial cell configuration resulting from this procedure is shown on the left in figure 6. The struts are clearly visible, embedded in the upper and lower vessel wall. SMC agents (blue) are lined by smaller internal elastic lamina (IEL) agents which are absent from the vessel wall region where the strut has penetrated.

15

## 5.2 Qualitative assessment of simulation results

We have run the simulation for an equivalent of 72 days (1700 time steps with $\Delta t = 1h$ for the SMC model) for both a bare metal stent and a drug eluting stent. In the current 2D implementation of the model, stent deployment results in laceration of the internal elastic lamina (as is observed in vivo) allowing proliferation of smooth muscle cells into the vessel lumen. These preliminary results demonstrate neointimal growth (proliferation of smooth muscle cells) in response to stent-induced injury. If we compare the output from immediately after stent deployment with that of 28 days later (Figure 6) it is apparent that the developing neointima causes a reduction in lumen diameter and an increase in wall shear stress. Because the SMC ruleset dictates that SMC agent proliferation is inhibited by high shear, once the neointimal growth causes shear stress to increase past a threshold, an equilibrium is reached and no more proliferation occurs. This fits nicely with biological theory which asserts that a vessel remodels in response to changes in haemodynamic forces, until those forces are normalised [21].

The proliferative response is reduced in the presence of drug; at the simulation endpoint (72 days), average neointimal thickness at the strut site in the absence of drug was $0.206 \pm 0.005$ mm versus $0.192 \pm 0.001$ mm in the presence of drug (Figure 7).

This trend was confirmed by examining the 'Normalised Peak Absolute Growth Fraction (NPAGF)'. This is defined as:

$$\text{NPAGF}(t) = \frac{r_{\text{M-phase}}(t)}{N_{\text{cells}}(t)} \max_{s \geq 0} r_{\text{M-phase}}(s) \, ,$$

i.e. the product of growth fraction $r_{\text{M-phase}}$ (Percentage of cells in M Phase/100) and total cell number $N_{\text{cells}}$, divided by the maximum value of the growth fraction across the series (Figure 7). The present data suggests that peak proliferation occurs at approximately 22 days in the presence of drug, and 20 days in the absence of drug. As our cell cycle dynamics and bulk flow parameters are based on porcine data, this second value agrees well with the findings of Schwartz *et al* [24] who derived the NPAGF for the rat, pig and human based on their experimental data and found the peak for the porcine series to be approximately 20 days.

## 5.3 Sensitivity Analysis

The single kernels have been singularly validated and their sensitivity with respect to model dependent parameters has been investigated. We remark that,
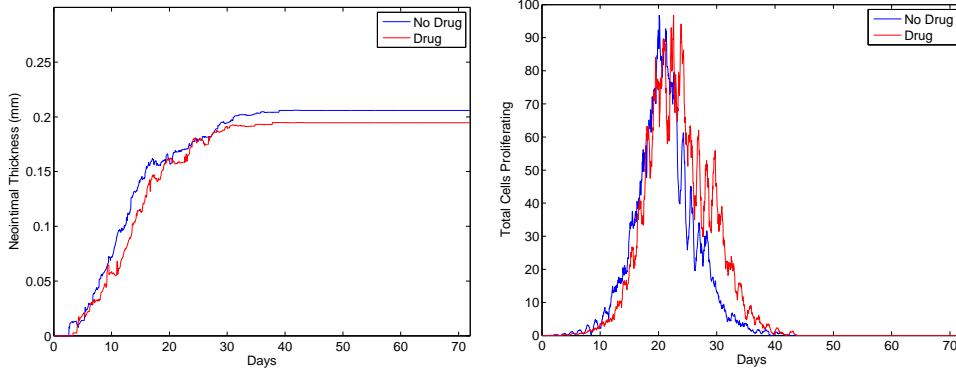
Figure 7. Left: Neointimal thickness at 72 days is reduced in the presence of anti-proliferative drug eluted from the stent strut. Right: If Normalised Peak Proliferation is considered, a single peak of proliferation occurs at 20 days in the absence of drug whereas in the presence of anti-proliferative drug, peak proliferation occurs at 22 days
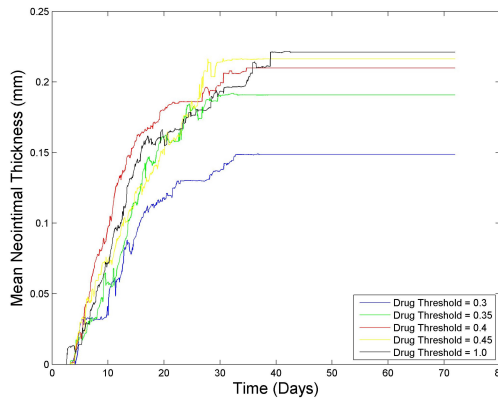


Figure 8. Sensitivity analysis: Drug Concentration effect. By varying the threshold of drug concentration at which SMC agent proliferation is inhibited, the degree of neointima formed by 72 days is modified.

given the structure of the MUSCLE framework, it is inherently simple to perform further sensitivity studies, for the global CxA setup with respect to key parameters of the single kernels. As an example, we investigated the threshold of drug concentration at which SMC agents change from a proliferative to quiescent phenotype, tunable by changing a single parameter in the global CxA setup. Figure 8 shows the relationship between this threshold and the amount of neointima present at seventy two days. Sensitivity analyses using different spatial resolutions for individual kernels can be also easily implemented.

17

In this particular case, the heaviest computational cost was represented by the bulk flow model, due to the fine resolution employed in the vessel (which was discretized using $O(10^3)$ nodes in 2D), in order to resolve sufficiently well the hydrodynamics near the walls. SMC and DD had a negligible cost, for each integration step. Note that the difference in cost can be reduced, e.g. using grid refinement approaches, and/or parallel codes. Investigating optimization techniques was not in the scopes of the present paper. However, an important practical remark is that the MUSCLE library builds the multiscale coupling environment independently from the instances of single scale models. In other words, It is completely flexible with respect to including newly developed single scale models, as well as handling distributed computing [13].

## 6   Conclusions and Outlook

We have shown how Complex Automata methodology can be applied in a challenging multiscale model of in-stent restenosis. In particular, we describe implementation of the coupling of three different subprocesses which operate on different time scales. The model has been realised employing a CxA-dedicated coupling library (MUSCLE), and preliminary results demonstrate that the CxA model can be successfully implemented within this framework. This first realisation of the coupled CxA is an important milestone on the journey towards a full multiscale model of in-stent restenosis.

Although individual models are at a relatively early stage and the current CxA is simplistic in nature, certain emergent behaviours are already apparent. For example, proliferation begins in response to injury, peaking at approximately 20 days following deployment in the absence of drug (Figure 7). We are currently in the process of running additional simulation series, to validate the trends emerging from the CxA against a biological data-set obtained from *in vivo* and *in vitro* experimentation using stented porcine arteries. In particular, we aim to characterize restenosis behaviour as a function of injury index [11] and to investigate the positive correlation between injury and restenosis.

It is important to remark that, although the two dimensional CxA model provides us with a tool for testing simple hypotheses (e.g. regarding the relationship between stent geometry, the cellular response to injury and the influence of haemodynamic forces), in order to evaluate realistic stent designs, however, it is necessary to run three dimensional simulations. This is part of an ongoing project, in which MUSCLE is being used to couple three dimensional versions of the bulk flow, SMC and drug diffusion kernels, and additionally, a

thrombus kernel. Future developments will require as well development of the single scale kernels. For example, implementation of more complex rulesets, to allow modeling of intercellular signalling pathways and the effects of deep injury, and a full pulsatile flow model for a more realistic local hydrodynamics. Moreover, the current CxA can be improved further by including extra kernels to model processes such as thrombus formation, endothelial loss and regrowth.

# References

[1] The Multiscale Coupling Library and Environment (MUSCLE). Sources and Documentation available at `http://muscle.berlios.de`.

[2] A.N.M. Artoli, A.G. Hoekstra, and P.M.A. Sloot. Mesoscopic simulations of systolic flow in Human abdominal aorta. *Journal of Biomechanics*, 39(5):873–884, 2006.

[3] L. Axner, A.G. Hoekstra, A. Jeays, P.V. Lawford, R. Hose, and P.M.A. Sloot. Simulations of time harmonic blood flow in the Mesenteric Artery: comparing finite element and lattice Boltzmann methods. *Biomedical Engineering Online*, 8(1):23–28, 2009.

[4] B. Chopard and M. Droz. *Cellular Automata Modeling of Physical Systems*. Cambridge University Press, Cambridge, 1998.

[5] B. Chopard, J.-L Falcone, R. Razakanirina, A.G. Hoekstra, and A. Caiazzo. On the collision-propagation and gather-update formulations of a cellular automata rule. In *Proceedings of ACRI 2008, LNCS 5191*, pages 144–251. Springer-Verlag Berlin Heidelberg, 2008.

[6] C.J. Dean, A.C. Morton, N.D. Arnold, D.R. Hose, D.C. Crossman and J. Gunn. Relative importance of the components of stent geometry to stretch induced in-stent neointima formation. *Heart*, 91:1603–1604, 2005.

[7] D. Evans, P. Lawford, J. Gunn, D. Walker, R. Hose, R. Smallwood, B. Chopard, M. Krafczyk, J. Bernsdorf, and A.G. Hoekstra. The application of multiscale modelling to the process of development and prevention of stenosis in a stented coronary artery. *Phil. Trans. Roy. Soc. A*, 366:3343–3360, 2008.

[8] A. Farb, G. Sangiorgi, A.J. Carter, M.W. Virginia, D.E. William, S.S. Robert, and V.Renu. Pathology of acute and chronic coronary stenting in humans. *Circulation*, 99(1):44–52, 1999.

[9] J.S. Forrester, M. Fishbein, R. Helfant, and J. Fagin. A paradigm for restenosis based on cell biology: clues for the development of new preventive therapies. *J Am Coll Cardiol*, 17(3):758–769, 1991.

[10] M. Gay, L.T. Zhang. Numerical studies on fluid–structure interactions of stent deployment and stented arteries. Engnr. with Comp., 25:61–72, 2009.

[11] J. Gunn, N. Arnold, K.H. Chan, L. Shepherd, D.G. Cumberland, and D.C. Crossman. Coronary artery stretch versus deep injury in the development of in-stent neointima. *Heart*, 88(4):401–5, 2002.

[12] J.H. Haga, Y.S. Li, and S. Chien. Molecular basis of the effects of mechanical stretch on vascular smooth muscle cells. *J. Biomech.*, 40(5):947–960, 2006.

[13] J. Hegewald, M. Krafczyk, A.G. Tölke J., Hoekstra, and B. Chopard. An agent-based coupling platform for complex automata. In *Proceedings of 8th ICCS, LNCS 5102*, pages 227–233. Springer, Berlin, Heidelberg, 2008.

[14] A. G. Hoekstra, E. Lorenz, J.-L. Falcone, and B. Chopard. Towards a complex automata formalism for multi-scale modeling. *Int. J. Mult. Comp. Eng.*, 5:491–502, 2007.

[15] A.G. Hoekstra, J.-L. Falcone, A. Caiazzo, and B. Chopard. Multi-scale modeling with cellular automata: The complex automata approach. In *Proceedings of ACRI 2008, LNCS 5191*, pages 192–199. Springer-Verlag, Berlin, Heidelberg, 2008.

[16] A.G. Hoekstra, E. Lorenz, J.L. Falcone, and B. Chopard. Towards a complex automata framework for multi-scale modeling: Formalism and the scale separation map. In *Proceedings of 7th ICCS, LNCS 4487*, pages 922–930. Springer-Verlag, Berlin, Heidelberg, 2007.

[17] C.-W. Hwang, D. Wu, and E.R. Edelman. Physiological transport forces govern drug distribution for stent-based delivery. *Circulation*, 104:600–605, 2001.

[18] A.D. Jeays, P.V. Lawford, R. Gillott, P. Spencer, D.C. Barber, K.D. Bardhan and D.R. Hose. Characterisation of the haemodynamics of the superior mesenteric artery. *Journal of Biomechanics*, 40:1916–1926, 2007.

[19] H.Kitano. Computational systems biology. *Nature*, 420:206–210, 2002.

[20] A.D. Levin, N. Vukmirovic, C.-W. Hwang, and E.R. Edelman. Specific binding to intracellular proteins determines arterial transport properties for rapamycin and paclitaxel. *PNAS*, 101:9463–9467, 2004.

[21] Y.S. Li, J.H. Haga, and S.Chien. Molecular basis of the effects of shear stress on vascular endothelial cells. *J. Biomech.*, 38(10):1949–1971, 2005.

[22] A. Morton, D. Crossman, and J. Gunn. The influence of physical stent parameters upon restenosis. *Pathologie Biologie*, 52:196–205, 2004.

[23] R. Ross. The pathogenesis of atherosclerosis: a perspective for the 1990s. *Nature*, 362(6423):801–809, 1993.

[24] R.S. Schwartz, A. Chu, W.D. Edwards, S.S. Srivatsa, R.D. Simari, J.M. Isner, and D.R. Holmes Jr. A proliferation analysis of arterial neointimal hyperplasia: lessons for antiproliferative restenosis therapies. *Int J Cardiol*, (53):71–80, 1996.

[25] P.M.A. Sloot and A.G. Hoekstra. Multiscale modeling in computational biology. *Briefings in Bioinformatics*, 11(1):142-152, 2010.

[26] J. Southern, J. Pitt-Francis, J. Whiteley, D. Stokeley, H. Kobashi, R. Nobes, Y. Kadooka, and D. Gavaghan. Multi-scale computational modelling in biology and physiology. *Progress in Biophysics and Molecular Biology*, 96:60–89, 2008.

[27] S. Succi. *The Lattice Boltzmann Equation for Fluid Dynamics and Beyond.* Oxford University Press, Oxford, 2001.

[28] D.C. Walker, G. Hill, S.M.Wood, R.H. Smallwood, J. Southgate. Agent-based computational modeling of epithelial cell monolayers: predicting the effect of exogenous calcium concentration on the rate of wound closure. *IEEE Transactions on NanoBioscience*, 3(3):153–163, 2004.

[29] D.C. Walker, J. Southgate, G. Hill, M. Holcombe, D.R. Hose, S.M. Wood, S. MacNeil.,R.H. Smallwood. The Epitheliome: modelling the social behaviour of cells. *Biosystems*, 76(1-3):89–100, 2004